https://doi.org/10.5194/acp-2019-908
Preprint. Discussion started: 11 November 2019
© Author(s) 2019. CC BY 4.0 License.

Atmospheric Chemistry and Physics Discussions

Urban organic aerosol composition in Eastern China differs from North to South: Molecular insight from a liquid chromatography-Orbitrap mass spectrometry study

Kai Wang[1,2,4], Ru-Jin Huang[1], Martin Brüggemann[3], Yun Zhang[2], Lu Yang[1], Haiyan Ni[1], Jie Guo[1], Meng Wang[1], Jiajun Han[5], Merete Bilde[4], Marianne Glasius[4], and Thorsten Hoffmann[2]

[1]State Key Laboratory of Loess and Quaternary Geology (SKLLQG), Center for Excellence in Quaternary Science and Global Change, and Key Laboratory of Aerosol Chemistry and Physics, Institute of Earth and Environment, Chinese Academy of Sciences, Xi'an 710061, China

[2]Institute of Inorganic and Analytical Chemistry, Johannes Gutenberg University Mainz, Duesbergweg 10−14, Mainz 55128, Germany

[3]Atmospheric Chemistry Department (ACD), Leibniz Institute for Tropospheric Research (TROPOS), Permoserstraße 15, 04318 Leipzig, Germany

[4]Department of Chemistry, Aarhus University, Langelandsgade 140, DK-8000 Aarhus C, Denmark

[5]Department of Chemistry, University of Toronto, 80 St. George Street, M5S3H6 Toronto, Canada

Corresponding Author: Ru-Jin Huang (rujin.huang@ieecas.cn) and Thorsten Hoffmann (t.hoffmann@uni-mainz.de)

https://doi.org/10.5194/acp-2019-908
Preprint. Discussion started: 11 November 2019
© Author(s) 2019. CC BY 4.0 License.

Atmospheric Chemistry and Physics Discussions

Abstract:

Particulate air pollution in China is influencing human health, ecosystem and climate. However, the chemical composition of particulate aerosol, especially of the organic fraction, is still not well understood. In this study, particulate aerosol samples with a diameter ⩽ 2.5 μm ($PM_{2.5}$) were collected in January 2014 in three cities located in Northeast, East and Southeast China, i.e., Changchun, Shanghai and Guangzhou, respectively. Organic aerosol (OA) in the $PM_{2.5}$ samples was analyzed by ultrahigh performance liquid chromatography (UHPLC) coupled to high-resolution Orbitrap mass spectrometry in both negative mode (ESI−) and positive mode electrospray ionization (ESI+). After a non-target screening including molecular formula assignments, compounds were classified into five groups based on their elemental composition, i.e., CHO, CHON, CHN, CHOS and CHONS. The CHO, CHON and CHN compounds present the dominant signal abundances of 81−99.7% in the mass spectra and the majority of these compounds were assigned to mono- and polyaromatics, suggesting that anthropogenic emissions are a large source of urban OA in all three cities. However, the chemical characteristics of these compounds varied among different cities. The degree of aromaticity and the number of polyaromatic compounds were significantly higher in samples from Changchun, which could be attributed to the large emissions from residential heating (i.e., coal combustion) during winter time in Northeast China. Moreover, the ESI− analysis showed higher H/C and O/C ratios for organic compounds in Shanghai and Guangzhou compared to samples from Changchun, indicating that OA in lower latitude regions of China experiences more intense photochemical oxidation processes. The majority of sulfur-containing compounds (CHOS and CHONS) in all cities were assigned to aliphatic compounds with low degrees of unsaturation and aromaticity. Again, samples from Shanghai and Guangzhou exhibit a larger chemical similarity but largely differ from those from Changchun.

1. Introduction

In the last decades, China has experienced rapid industrialization and urbanization accompanied by severe and persistent particulate air pollution (Huang et al., 2014; Sun et al., 2014; Ding et al., 2016; Song et al., 2018; Shi et al., 2019; Xu et al., 2019). These particulate air pollution extremes can not only influence the regional air quality and human health in China, but also lead to a global environmental problem due to long-distance transport of pollutants. To better understand the effects of air pollution on air quality and human health, chemical characterization of fine particle (particulate matter with an aerodynamic diameter of less than 2.5 μm, or $PM_{2.5}$) is crucial. However,

https://doi.org/10.5194/acp-2019-908
Preprint. Discussion started: 11 November 2019
© Author(s) 2019. CC BY 4.0 License.

Atmospheric Chemistry and Physics Discussions

the chemical composition of $PM_{2.5}$ in China is still poorly understood due to a wide variety of natural and anthropogenic sources as well as complex multiphase chemical reactions (Lin et al., 2012a; Huang et al., 2014; Ding et al., 2016; Wang et al., 2017; Wang et al., 2018; An et al., 2019; Wang et al., 2019a; Wang et al., 2019b). In particular, compared to the fairly well understood nature of the inorganic fraction of aerosol, the organic fraction, also named organic aerosol (OA), is considerably less comprehended in terms of chemical composition, corresponding precursors, sources and formation mechanisms (Huang et al., 2017).

During pollution events in China, OA accounts for as high as more than 50% of the total mass of fine particle (An et al., 2019). Chemical compounds in OA cover a large complexity of species including alcohols, aldehydes, carboxylic acids, imidazoles, organosulfates, organonitrates and polycyclic aromatic hydrocarbons (PAHs) (Lin et al., 2012a; Rincón et al., 2012; Kourtchev et al., 2014; Wang et al., 2018; Elzein et al., 2019; Wang et al., 2019a). Thus, the capacity of traditional analytical techniques is limited to identify the compounds in OA and the majority (> 70%) of OA has not been identified yet as specific compounds (Hoffmann et al., 2011). The insufficient knowledge of chemical composition of OA hinders a better understanding of the sources, formation and atmospheric processes of air pollution in China.

Recently, ultrahigh resolution mass spectrometry (UHRMS), such as Fourier transform ion cyclotron resonance mass spectrometry (FTICR−MS) and Orbitrap−MS, coupled with soft ionization sources (e.g., electrospray ionization (ESI) and atmospheric pressure chemical ionization (APCI)) have been introduced to elucidate the molecular composition of OA (Nizkorodov et al., 2011; Lin et al., 2012a; Lin et al., 2012b; Rincón et al., 2012; Noziere et al., 2015; Kourtchev et al., 2016; Tong et al., 2016; Tu et al., 2016; Brüggemann et al., 2017; Wang et al., 2017; Fleming et al., 2018; Laskin et al., 2018; Song et al., 2018; Wang et al., 2018; Brüggemann et al., 2019; Daellenbach et al., 2019; Ning et al., 2019; Wang et al., 2019a). Due to the two outstanding features of high resolving power and high mass accuracy, UHRMS can give precise elemental compositions of individual organic compounds. However, UHRMS studies on Chinese urban OA are very limited. Wang et al. (Wang et al., 2017) characterized OA in Shanghai and showed variations in chemical composition among different months and between daytime and nighttime. Our recent Orbitrap MS study (Wang et al., 2018) showed that wintertime OA in $PM_{2.5}$ collected in Beijing, China and Mainz, Germany were very different in terms of chemical composition. In contrast, for summertime OA from Germany and China, Brüggemann et al. (2019) found similar compounds and concentrations of terpenoid organosulfates in PM_{10}, demonstrating that biogenic emission can significantly affect OA composition at both locations. Ning et al. (2019) analyzed the OA collected

https://doi.org/10.5194/acp-2019-908
Preprint. Discussion started: 11 November 2019
© Author(s) 2019. CC BY 4.0 License.

Atmospheric Chemistry and Physics Discussions

in a coastal Chinese city (Dalian) and found that more organic compounds were identified in haze days compared to non-haze days. Nonetheless, since severe particulate pollution in China occurs on a large-scale, more UHRMS studies are needed to fully elucidate the chemical composition of OA in different Chinese cities.

In this study, $PM_{2.5}$ aerosol samples were collected in three Chinese cities, i.e., Changchun, Shanghai and Guangzhou, and their organic fraction was analyzed using ultra-high-performance liquid chromatography (UHPLC) coupled with Orbitrap−MS. The Chinese cities of Changchun, Shanghai and Guangzhou are located in the Northeast, East and Southeast of China, which are major populated regions in China with a population of 7.5, 24 and 15 million, respectively. The geographic locations of these three cities cover a large latitude spanning from 23.12° N to 43.53° N resulting in different meteorological conditions, including intensity and duration of sunlight, average daily temperature and monsoon climate. In addition, the industrial structure, energy consumption and energy sources in these three cities are different, which can cause difference in anthropogenic emissions, and thus, influence the chemical composition of the urban OA. For example, OA is strongly affected by residential coal combustion during winter in Northeast China (Huang et al., 2014; An et al., 2019). Therefore, this study presents a comprehensive overview of chemical composition of OA in three representative Chinese cities during pollution episodes, which eventually can improve our understanding of OA effects on climate and public health and also provide a chemical database for haze mitigation strategies in China.

2. Experimental

2.1 $PM_{2.5}$ samples

Three 24−h integrated urban $PM_{2.5}$ samples were collected during severe haze pollution events with daily average $PM_{2.5}$ mass concentration higher than 115 μg m^{-3} in each of the three Chinese cities: Changchun (43.54° N, 125.13° E, 1.5 m above the ground), Shanghai (31.30° N, 121.50° E, 20 m above the ground) and Guangzhou (23.07° N, 113.21° E, 53 m above the ground), which are located in the Northeast, East and Southeast regions of China, respectively (see Fig. 1). Samples in Changchun were collected on 4, 24 and 29 of January 2014 with $PM_{2.5}$ mass concentrations of 185−222 μg m^{-3}, samples in Shanghai were collected on 1, 19 and 20 of January 2014 with $PM_{2.5}$ mass concentrations of 159−172 μg m^{-3} and samples in Guangzhou were collected on 5, 6 and 11 of January 2014 with $PM_{2.5}$ mass concentrations of 138−152 μg m^{-3}. Further details (e.g., the daily average concentrations of $PM_{2.5}$, SO_2, NO_2, CO and O_3, and average temperature during sampling dates) are presented in Table S1. All $PM_{2.5}$ samples were collected on prebaked quartz-fiber filters

https://doi.org/10.5194/acp-2019-908
Preprint. Discussion started: 11 November 2019
© Author(s) 2019. CC BY 4.0 License.

Atmospheric Chemistry and Physics Discussions

(20.3×25.4 cm) using a high-volume $PM_{2.5}$ sampler at a flow rate of 1.05 m^3 min^{-1} (Tisch Environmental, USA) and at each sampling site field blanks were taken. After sample collection, filters were stored at −20 °C until analysis.

2.2 Sample analysis

Detailed description on the filter sample extraction and UHPLC−Orbitrap MS analysis can be found in our previous studies (Wang et al., 2018; Wang et al., 2019a). Briefly, a part of the filters (around 1.13 cm^2, corresponding to about 600 µg particle mass in each extracted filter) was extracted three times with 1.0−1.5 mL of acetonitrile-water (8/2, v/v) in an ultrasonic bath. The extracts were combined, filtered through a 0.2 µm Teflon syringe filter and evaporated to almost dryness under a gentle nitrogen stream. Finally, the residue was redissolved in 1000 µL acetonitrile-water (1/9, v/v) to reach the total particulate mass concentration of around 600 µg mL^{-1} for the following analysis.

The analytes were separated using a Hypersil Gold column (C18, 50 x 2.0 mm, 1.9 µm particle size) with mobile phases consisting of (A) 0.04% formic acid and 2% acetonitrile in MilliQ water and (B) 2% water in acetonitrile. Gradient elution was applied with the A and B mixture at a flow rate of 500 µL min^{-1} as follows: 0−1.5 min 2% B, 1.5−2.5 min from 2% to 20% B (linear), 2.5−5.5 min 20% B, 5.5−6.5 min from 20% to 30% B (linear), 6.5−7.5 min from 30% to 50% B (linear), 7.5−8.5 min from 50% to 98% B (linear), 8.5−11.0 min 98% B, 11.0−11.05 min from 98% to 2% B (linear), and 11.05−11.1 min 2% B. The Q Exactive Hybrid Quadrupole-Orbitrap MS was equipped with a heated ESI source at 120 °C, applying a spray voltage of −3.3 kV and 4.0 kV for negative ESI mode (ESI−) and positive ESI mode (ESI+), respectively. The mass scanning range was set from m/z 50 to 500 with a resolving power of 70,000 @ m/z 200. The Orbitrap MS was externally calibrated before each measurement sequence using an Ultramark 1621 solution (Sigama−Aldrich, Germany) providing mass accuracy of the instrument lower than 3 ppm. Each sample was measured in triplicate with an injection volume of 10 µL.

2.3 Data processing

A non-target peak picking software (SIEVE®, Thermo Fisher Scientific, Germany) was used to find significant peaks in the LC-MS dataset and to calculate all mathematically possible chemical formulas for ions signals with a sample-to-blank abundance ratio ⩾10 using a mass tolerance of ± 2 ppm. The permitted maximum elemental number of atoms was set as follows: ^{12}C (39), ^{1}H (72), ^{16}O (20), ^{14}N (7), ^{32}S (4), ^{35}Cl (2) and ^{23}Na (1) (Kind and Fiehn, 2007; Lin et al., 2012a; Wang et

https://doi.org/10.5194/acp-2019-908
Preprint. Discussion started: 11 November 2019
© Author(s) 2019. CC BY 4.0 License.

Atmospheric Chemistry and Physics Discussions

al., 2018). To remove the chemically unreasonable formulas, further constraint was applied by setting H/C, O/C, N/C, S/C and Cl/C ratios in the ranges of 0.3−3, 0−3, 0−1.3, 0−0.8 and 0−0.8 (Kind and Fiehn, 2007; Lin et al., 2012a; Rincón et al., 2012; Wang et al., 2018; Zielinski et al., 2018), respectively. For chemical formula $C_cH_hO_oN_nS_sCl_x$, the double bond equivalent (DBE) was calculated by the equation: DBE = (2c + 2 – h – x + n) / 2, and the aromaticity equivalent (X_C) as a modified index for aromatic compounds was obtained using the equation: Xc = [3(DBE – (p × o + q × n)) – 2] / [DBE – (p × o + q × n)], where p and q, respectively, refer to the fraction of oxygen and sulfur atoms involved in the π-bond structure of a compound. Xc ⩾ 2.50 and Xc ⩾ 2.71 have been suggested as unambiguous minimum criteria for the presence of monoaromatics and polyaromatics, respectively (Yassine et al., 2014). Further details on the data processing can be found in our previous studies (Wang et al., 2018; Wang et al., 2019a) and is also presented in the Supporting Information (SI).

3. Results and discussion

3.1 General characteristics

The main purpose of this study was to tentatively identify and compare the chemical composition of organic compounds in the $PM_{2.5}$ samples collected in the three Chinese cities: Changchun, Shanghai and Guangzhou during pollution episodes. The number of organic compounds detected in each city and the abundance-weighted average values of molecular mass (MM_{avg}), elemental ratios, DBE and Xc for each subgroup are listed in Table 1. It should be noted that in this study we focus solely on organic compounds with elevated signal abundances, and thus, presumably rather high concentrations. In contrast to our previous study (Wang et al., 2018), compounds with low concentrations were excluded by increasing the reconstitution volume from 500 μL to 1000 μL, reducing the sample injection volume from 20 μL to 10 μL, and increasing the sample-to-blank ratio from 3 to 10 during data processing.

Overall, 416−769 and 687−2943 organic compounds in different samples were determined in ESI− and ESI+, respectively. The largest number of organic compounds was observed in Changchun samples in both ESI− and ESI+, indicating that OA collected during winter season in Northeast China was more complex compared to urban OA in East and Southeast China. This increased number of compounds can possibly be explained by the large residential coal combustion emissions in winter in North China (Huang et al., 2014; Song et al., 2018; An et al., 2019). In addition, ambient temperatures were lowest during the sampling period in Changchun (i.e., −14 ℃ to −9 ℃, Table S1), which likely led to a decreased boundary layer height and therefore enhanced accumulation of

https://doi.org/10.5194/acp-2019-908
Preprint. Discussion started: 11 November 2019
© Author(s) 2019. CC BY 4.0 License.

Atmospheric Chemistry and Physics Discussions

pollutants and enhanced formation of secondary organic aerosol through for example gas-to-particle partitioning.

As shown in Table 1, the abundance-weighted average values of MM_{avg}, H/C and O/C ratio of the total assigned formulas for Changchun samples decteced in negative mode (Changchun−) are 169, 1.03 and 0.58, respectively, which are significantly lower compared to those for Shanghai− (MM_{avg} = 176, H/C = 1.05 and O/C = 0.69) and for Guangzhou− (MM_{avg} = 183, H/C = 1.14 and O/C = 0.74). On the contrary, the aromaticity equivalent Xc for organics detected in Changchun−, Xc(Changchun–) = 2.13, is higher than that for Shanghai−, Xc(Shanghai–) = 1.92, and Guangzhou− , Xc(Guangzhou–) = 1.65. These observations indicate that urban OA in Northeast China features a lower degree of oxidation and a higher degree of aromaticity compared to urban OA in East and Southeast China. The different chemical composition of the samples is probably caused by the rather low ambient temperatures and decreased photochemical processing of organic compounds in Northeast China, slowing down oxidation processes and leading to a larger number of PAHs, which are mainly emitted from coal burning (Huang et al., 2014; Song et al., 2018).

Figure 1 shows the reconstructed mass spectra of organic compounds detected in ESI− and ESI+. It should be noted that uncertainties always exist when comparing signal abundances of organic compounds due to their different ionization efficiencies and the gradient elution applied in the separation method (Perry et al., 2008). In this study, we assume that all organic compounds have roughly the same mass spectral response and we compare the peak abundances of organic compounds among the different samples. A major fraction organic species detected in ESI− are attributed to CHO− and CHON−, accounting for 30−42% and 39−55% in terms of peak abundance, respectively, and comprising 39-45% and 23-33% in terms of peak numbers, respectively. This is consistent with previous studies on Chinese urban OA by Wang et al. (2017 and 2018) and Brüggemann et al. (2019). Comparing the organic compounds detected in ESI− for the three cities, 139 formulas were observed in all cities as common formulas (Fig. 2a), accounting for 35−51% and 78−87% of all assigned formulas in terms of peak numbers and peak abundance, respectively. Despite the above-mentioned differences in chemical composition for OA from Changchun compared to OA from Shanghai and Guangzhou, these results demonstrate that still a large number of common organic compounds exist in Chinese urban OAs collected in different cities, in particular for organics with higher signal abundances. Furthermore, as shown by the pie chart in Fig. 2b, these common formulas are dominated by CHON− and CHO−, accounting for 59% and 33% of the total common formulas in terms of peak abundance, respectively.

https://doi.org/10.5194/acp-2019-908
Preprint. Discussion started: 11 November 2019
© Author(s) 2019. CC BY 4.0 License.

Atmospheric Chemistry and Physics Discussions

As it is commonly known, ESI exhibits different ionization mechanisms in negative and positive ionization modes. While ESI− is especially sensitive to deprotonatable compounds (e.g., organic acids), ESI+ is more sensitive to protonatable compounds (e.g., organic amines) (Ho et al., 2003). Due to the different ionization mechanisms, clear differences were observed in the mass spectra (Fig. 1) and chemical characteristics (Table 1) from ESI− and ESI+ measurements. For example, CHO compounds were preferentially detected in ESI−, accounting for a relatively large fraction of 30−42% of all detected compounds, compared to merely 4−13% for such CHO compounds in ESI+. In contrast, CHN compounds were only observed in ESI+, yielding a rather large peak abundance fraction of 40−71%. This observation indicates that most CHO compounds with high concentrations are probably organic acids, whereas the majority of CHN compounds likely belong to the group of organic amines, which is in good agreement with previous studies (Lin et al., 2012a; Wang et al., 2017; Wang et al., 2018). Organic compounds in ESI+ are dominated by CHN+ and CHON+ compounds in terms of both peak number and peak abundance and these compounds are characterized by rather high H/C ratio and low O/C ratios (Table 1), indicating a low degree of oxidation. The Venn diagram presented for ESI+ measurements in Fig. 2a shows that out of a total of 383−679 formulas, 168 formulas were found in samples from all three cities. Such common formulas, thus, account for 25−44% and 65−90% of all assigned formulas in terms of peak numbers and peak abundance, respectively. Among these common formulas, CHN+ and CHON+ exhibit the highest abundance fractions of 61% and 35%, respectively (Fig. 2b).

In the following, we will compare and discuss the chemical properties in detail for the three cities, including degrees of oxidation, unsaturation and aromaticity of each organic compound class (i.e., CHO, CHON, CHN, CHOS and CHONS). It should be noted that the chlorine-containing compounds were not discussed in this study due to the very low MS signal abundance.

3.2 CHO compounds

CHO compounds have been widely observed in urban OA, accounting for a substantial fraction (8−67%) of OA (Rincón et al., 2012; Tao et al., 2014; Wang et al., 2017; Wang et al., 2018). Previous studies have shown that a large fraction of CHO compounds in urban OA is composed of organic acids, containing deprotonatable carboxyl functional groups, which are detected preferentially in negative ionization mode when using ESI−MS. As shown in Table 1, a total of 346, 164, and 196 CHO− compounds were detected in ESI− in the OA samples collected in Changchun, Shanghai and Guangzhou, accounting for 30%, 40% and 42% of the overall peak abundance in each sample, respectively. Out of all detected compounds, 52 common CHO−

https://doi.org/10.5194/acp-2019-908
Preprint. Discussion started: 11 November 2019
© Author(s) 2019. CC BY 4.0 License.

Atmospheric Chemistry and Physics Discussions

formulas were observed for all cites, accounting for 13−17% and 74−88% of all identified CHO− formulas in terms of numbers and abundance, respectively.

Despite this similarity, OA samples from Changchun− (i.e. in negative ionization mode) exhibit certain differences compared to samples from Shanghai− and Guangzhou−. The average H/C values for CHO− compounds are in a similar range for the three locations (i.e., 0.96−1.10), however, the average O/C values for O/C(Shanghai−) = 0.59 and O/C(Guangzhou−) = 0.65 are rather high compared to the average O/C ratio for Changchun−, O/C(Changchun–) = 0.41. Furthermore, the van Krevelen diagram in Fig. S1 also shows that more CHO− compounds with higher O/C ratios were found in Shanghai− and Guangzhou− compared to Changchun−. Altogether, these results indicate that CHO− compounds in urban OA from East and Southeast China experienced more intense oxidation and aging processes.

Similarly, as shown in Fig. 3, the abundance-weighted average molecular formulas for CHO− compounds in Changchun−, Shanghai– and Guangzhou− are $C_{8.58}H_{7.86}O_{3.22}$ (MM_{avg}(Changchun–) = 162), $C_{8.01}H_{7.27}O_{4.22}$ (MM_{avg}(Shanghai–) = 171) and $C_{7.70}H_{8.04}O_{4.48}$ (MM_{avg}(Guangzhou–) = 172), respectively. Again, these average formulas show that CHO− compounds from OA in Shanghai− and Guangzhou− experienced more intense oxidation processes, indicated by the larger abundance-weighted MM_{avg} with a higher degree of oxygenation. In contrast, CHO− compounds from OA samples in Changchun− exhibit a lower abundance-weighted MM_{avg} with a decreased oxygen content.

Besides oxygenation, the aromaticity of the detected CHO− compounds exhibits remarkable differences in these three cities. In all cities, the CHO– compounds with high peak abundance were mainly assigned to monoaromatics with $2.5 \leqslant Xc < 2.7$ (purple circles in Fig. 3) in the region of 7−12 carbon atoms per compound and DBE values of 5−7. The fraction of monoaromatics in total CHO– compounds is 67% in Changchun, which is higher compared to 64% in Shanghai and 49% in Guangzhou. In addition, 14% of CHO− compounds in Changchun were identified as polyaromatic compounds with $Xc \geqslant 2.7$ (red circles in Fig. 3), which are significantly higher than 8% in Shanghai and 4% in Guangzhou. These observations indicate that CHO− compounds in the three Chinese cities are highly affected by aromatic precursors (e.g., benzene, toluene and naphthalene), in particular for Changchun aerosol samples.

Besides the monoaromatics and polyaromatics, the rest of the detected CHO− compounds was assigned to aliphatic compounds with an Xc lower than 2.5 (grey circles in Fig. 3). Interestingly, these aliphatic compounds account for about 47% of CHO− compounds for Guangzhou− samples

https://doi.org/10.5194/acp-2019-908
Preprint. Discussion started: 11 November 2019
© Author(s) 2019. CC BY 4.0 License.

Atmospheric Chemistry and Physics Discussions

in terms of peak abundance, whereas samples from Changchun− and Shanghai− exhibit only rather small fractions of such CHO− compounds, i.e., 19% and 28%, respectively. Such aliphatic compounds are commonly derived from biogenic precursors (Kourtchev et al., 2016) and vehicle emission (Tao et al., 2014; Wang et al., 2017) and/or generated by intense oxidation processes of aromatic precursors, indicating the different biogenic and anthropogenic emission sources and chemical reaction processes for OAs in the three cities.

In addition, through mass spectrometric analysis of individual compounds, we find that for the Changchun− samples, formulas of $C_8H_6O_4$, $C_7H_6O_2$, $C_7H_6O_3$, $C_8H_8O_2$, and $C_8H_8O_3$ with DBE values of 6, 5, 5, 5, and 5 dominate the assigned CHO formulas with respect to peak abundance. According to previous studies, $C_8H_6O_4$, $C_7H_6O_2$ and $C_7H_6O_3$ are suggested to be phthalic acid, benzoic acid and monohydroxy benzoic acid, respectively, which are derived from naphthalene (Kautzman et al., 2010; Riva et al., 2015; Wang et al., 2017; He et al., 2018; Huang et al., 2019). $C_8H_8O_2$ and $C_8H_8O_3$ are likely 4-hydroxy acetophenone and 4-methoxybenzoic acid which could be derived from estragole (Lee et al., 2006; Pereira et al., 2014). For the Shanghai− samples, besides $C_8H_6O_4$, $C_7H_6O_3$ and $C_7H_6O_2$, formulas of $C_6H_8O_7$ and $C_9H_8O_4$ with DBE values of 3 and 6 were observed with high peak abundances. $C_6H_8O_7$ was identified as citric acid in the pollen sample and mountain particle sample in previous studies (Fu et al., 2008; Wang et al., 2009; Jung and Kawamura, 2011) and $C_9H_8O_4$ are probably homophthalic acid derived from e.g. estragole (Pereira et al., 2014). For the Guangzhou− samples, besides the formulas of $C_8H_6O_4$ and $C_6H_8O_7$ discussed above, $C_4H_6O_4$ and $C_4H_6O_5$ with low DBE values of two were detected with high abundances and are suggested to be succinic acid and malic acid, respectively (Claeys et al., 2004; Wang et al., 2017).

3.3 CHON compounds

A large amount of nitrogen-containing organic compounds was detected in these three cities, accounting for 39−55% and 25−47% of total peak abundance detected in ESI− and ESI+, respectively. Out of all detected compounds, 51 common CHON− and 89 common CHON+ formulas were observed in all cities, accounting for 90−96% and 61−75% of all CHON compounds detected in ESI− and ESI+ in terms of peak abundance, respectively. This large fraction of common formulas indicates that the chemical composition of CHON compounds with higher signal abundances, and thus, presumably high concentrations are quite similar in all three Chinese cities.

The CHON compounds were further classified into different subgroups according to their O/N ratios. As shown in Fig. 4, the majority (84−96%) of CHON− compounds exhibit O/N ratios $\geqslant 3$, allowing the assignment of one nitro ($-NO_2$) or nitrooxy ($-ONO_2$) group for these formulas, which

https://doi.org/10.5194/acp-2019-908
Preprint. Discussion started: 11 November 2019
© Author(s) 2019. CC BY 4.0 License.

Atmospheric Chemistry and Physics Discussions

are preferentially ionized in ESI− mode (Lin et al., 2012b; Wang et al., 2017; Song et al., 2018; Wang et al., 2018). CHON− formulas with O/N ratios ⩾ 4 suggest the presence of further oxygenated functional groups, such as a hydroxyl group (−OH) or a carbonyl group (C=O). 59% of CHON− compounds with O/N ratios ⩾ 4 were found in in Guangzhou−, which is significantly higher than 51% in Changchun− and 45% in Shanghai−, indicating that CHON− compounds in Southeast China show a higher degree of oxidation compared to those in Northeast and East China. Not surprisingly, CHON+ compounds generally exhibit lower O/N ratios (Fig. S2), as they probably contain reduced nitrogen functional group (e.g., amines) which are preferably detected in ESI+. As shown in Fig. S2, CHON+ compounds with O/N ratio of 1 are dominant in Changchun+, whereas CHON+ compounds in Shanghai+ and Guangzhou+ show a broader range of O/N ratios from 1 to 3. Moreover, the average O/C ratios (0.27−0.45) in Shanghai+ and Guangzhou+ (Table 1) are much greater than that (0.19) in Changchun+. Consistent with the observations for CHO compounds, these results indicate again that CHON+ compounds in the OA of East and Southeast China experienced more intensive photooxidation, which is probably due to the higher intensity and longer duration of sunlight in lower latitude parts of China during winter.

Figure 5 shows the DBE versus C number of CHON− compounds for the three cities. The majority of CHON− compounds lie in the region of 5−15 C atoms and 3−10 DBEs. 67% of CHON− compounds were assigned to mono or polyaromatics in Shanghai−, which is significant higher than 52% in Guangzhou− and 55% in Changchun−. Additionally, the average DBE value for Shanghai−, DBE_{avg}(Shanghai−) = 5.67, is larger than corresponding values for Changchun− and Guangzhou− with DBE_{avg}(Changchun−) = 5.24 and DBE_{avg}(Guangzhou−) = 5.56, respectively. These observations indicate that CHON− compounds are dominated with aromatic compounds in all cities, while they have higher degree of aromaticity and unsaturation in Shanghai− compared with those in Changchun− and Guangzhou−. The abundance-weighted average molecular formulas for CHON− compounds in Changchun−, Shanghai− and Guangzhou− are $C_{7.10}H_{6.76}O_{3.56}N_{1.03}$, $C_{7.07}H_{6.03}O_{3.80}N_{1.24}$ and $C_{7.12}H_{6.36}O_{3.99}N_{1.24}$, respectively, showing that CHON− formulas in Shanghai− and Guangzhou− contain more O and N atoms on average than those for Changchun−. Formulas of $C_6H_5O_3N_1$, $C_6H_5O_4N_1$, $C_7H_7O_3N_1$, $C_7H_7O_4N_1$, $C_8H_9O_3N_1$, and $C_8H_9O_4N_1$ were detected with the highest abundance in all cities. These molecular formulas are in line with nitrophenol or nitrocatechol analogs, which have been identified in a previous urban OA study (Wang et al., 2017). Furthermore, these nitrooxy-aromatic compounds were shown to enhance light absorbing properties of OA (Laskin et al., 2015; Lin et al., 2015). In addition, it should be noted that the Xc values for $C_6H_5O_4N_1$, $C_7H_7O_4N_1$ and $C_8H_9O_4N_1$ were calculated to be lower than 2.5, suggesting

https://doi.org/10.5194/acp-2019-908
Preprint. Discussion started: 11 November 2019
© Author(s) 2019. CC BY 4.0 License.

Atmospheric Chemistry and Physics Discussions

that the fraction of aromatics in CHON− compounds was underestimated. This is because that for nitrocatechol analogs with formulas of $C_6H_5O_4N_1$, $C_7H_7O_4N_1$ and $C_8H_9O_4N_1$, only one oxygen atom is involved in the π-bond structure corresponding to the p value of 0.25 in the Xc calculation equation, which is lower than the p value of 0.5 applied for the Xc calculation in this study. The diagram of DBE versus C number for CHON+ compounds observed in the three locations (presented in Fig. S3 in SI) shows that more aromatic CHON+ compounds with relatively lower degree of oxidation were assigned in Changchun+ samples compared to Shanghai+ and Guangzhou+ samples.

3.4 CHN+ compounds

205−696 CHN+ compounds were detected in ESI+, which are likely amines according to previous studies (Rincón et al., 2012; Wang et al., 2017; Wang et al., 2018). The number of CHN+ compounds accounts for 24%, 36% and 30% of the total organic compounds in Changchun+, Shanghai+ and Guangzhou+, respectively, whereas the peak abundance of these compounds accounts for 40%, 71% and 62%, respectively. Comparing the CHN+ compounds for the three cities, 58 common CHN+ formulas were observed in all cities, which contribute to as much as 83−98% of the total abundance of CHN+ formulas. This large percentage indicates that CHN+ compounds with presumably high concentrations in Changchun+, Shanghai+ and Guangzhou+ exhibit similar chemical composition. However, again OA samples from Changchun show some distinct differences to samples from Guangzhou and Shanghai, giving the smallest ratio for number and peak abundance of CHN+ compounds.

A van Krevelen diagram of CHN+ compounds detected in the three samples is shown in Fig. 6, illustrating H/C ratios as a function of N/C ratio. In this plot, major parts of the CHN+ compounds are found in a region, which is constraint by H/C ratios between 0.5 and 2 and N/C ratios lower than 0.5. Moreover, the pie charts show that the majority (83−87%) of these CHN+ compounds can be assigned to mono- and polyaromatics with Xc $\geqslant$ 2.5. In addition, as shown in Table 1, the average DBE and Xc values of CHN+ compounds are the highest among all organic species. These observations imply that CHN+ compounds exhibit the highest degree of aromaticity of all organics in the Chinese urban OA samples, which is consistent with previous studies (Lin et al., 2012b; Rincón et al., 2012; Wang et al., 2018). Polyaromatic compounds with Xc $\geqslant$ 2.7 are displayed in the lower left corner of the van Krevelen diagram, accounting for 41% of CHN+ compounds detected in Changchun+, but merely for 9−10% in Shanghai+ and Guangzhou+. For example, formulas of $C_{11}H_{11}N_1$ (Xc = 2.7), $C_{10}H_9N_1$ (Xc = 2.7), and $C_{12}H_{13}N_1$ (Xc = 2.7), which are assigned

https://doi.org/10.5194/acp-2019-908
Preprint. Discussion started: 11 November 2019
© Author(s) 2019. CC BY 4.0 License.

Atmospheric Chemistry and Physics Discussions

to be naphthalene core structure-containing compounds, have relatively higher abundance in Changchun+ than in Shanghai+ and Guangzhou+. Moreover, the average DBE and Xc values of CHN+ compounds in Changchun+ are significantly higher than those in Shanghai+ and Guangzhou+, further indicating that CHN+ compounds in Changchun+ show a higher degree of aromaticity, which can be caused by large coal combustion emissions in the winter in Changchun. According to a previous smog chamber study (Laskin et al., 2010), most CHN+ aromatics are probably generated from biomass burning through the addition of reduced nitrogen (e.g., NH_3) to the organic molecules via imine formation reaction, indicating that biomass burning probably made a certain contribution to the formation of CHN+ compounds observed in the three urban OA samples in our study.

3.5 CHOS− compounds

In this study, 75−155 CHOS− compounds were observed, accounting for 10%, 12% and 14% of the total peak abundance of all organics in Changchun−, Shanghai− and Guangzhou−, respectively. Around 89−96% of these CHOS− compounds were found to fulfill the O/S $\geqslant$ 4 criterion allowing the assignment of at least one $-OSO_3H$ functional group, and thus, a tentative classification to organosulfates (OSs) (Lin et al., 2012a; Lin et al., 2012b; Tao et al., 2014; Wang et al., 2016; Wang et al., 2017; Wang et al., 2018; Wang et al., 2019a). OSs were shown to affect the surface activity and hygroscopic properties of the aerosol particles, leading to potential impacts on climate (Hansen et al., 2015; Wang et al., 2019a). Out of all formulas, 28 common CHOS− formulas were detected for the three sample locations, accounting for 39%, 68% and 65% of the CHOS− peak abundance in Changchun−, Shanghai− and Guangzhou−, respectively. However, 40 common CHOS− formulas were found between Shanghai− and Guangzhou−, accounting for 60−65% and 70−83% in terms of the CHOS− compounds number and peak abundance, respectively. This indicates that the chemical composition of the major CHOS− compounds of Shanghai− and Guangzhou− are quite similar, while they show significant chemical differences for samples from Changchun−.

Figure 7 shows the DBEs as a function of carbon number for all CHOS− compounds detected for the three cities. The CHOS− compounds exhibit a DBE range from 0 to 10 and carbon number range of 2−15. However, the majority of CHOS− compounds with elevated peak abundances concentrate in a region with rather low DBE values of 0−5. The average H/C ratios of CHOS– compounds are in the range of 1.56−1.85, and thus, higher than for any other compound class, whereas the average DBE values of 1.71−2.55 are the lowest among all classes. This indicates that CHOS− compounds in the OA from the three Chinese cities are characterized by a low degree of

https://doi.org/10.5194/acp-2019-908
Preprint. Discussion started: 11 November 2019
© Author(s) 2019. CC BY 4.0 License.

Atmospheric Chemistry and Physics Discussions

412 unsaturation. Moreover, the pie charts in Fig. 7 show that aliphatic compounds with Xc ⩽ 2.5 are
413 dominant in CHOS− compounds with a fraction of 96−99%, which is significantly higher than that
414 (13−48%) for CHO, CHON and CHN species. Aliphatic CHOS− compounds with C ⩽ 10 can be
415 formed from biogenic and/or anthropogenic precursors (Hansen et al., 2014; Glasius et al., 2018;
416 Wang et al., 2019a), such as $C_2H_4O_6S_1$ (derived from glyoxal) (Lim et al., 2010; McNeill et al.,
417 2012), $C_3H_6O_6S_1$ (derived from isoprene) (Surratt et al., 2007) and $C_8H_{16}O_4S_1$ (derived from α-
418 pinene) (Surratt et al., 2007). However, more CHOS− compounds with C > 10 and with DBEs
419 lower than 1 are observed in Changchun−, such as $C_{14}H_{28}O_5S_1$, $C_{13}H_{26}O_5S_1$, $C_{12}H_{24}O_5S_1$,
420 $C_{11}H_{22}O_5S_1$ and $C_{11}H_{20}O_6S_1$. These high-carbon-number-containing CHOS− compounds are likely
421 formed from long-alkyl-chain compounds with less oxygenated functional groups, which were
422 previously suggested to be emitted from traffic (Tao et al., 2014) or derived from sesquiterpene
423 emissions (Brüggemann et al., 2019). However, as sesquiterpene emissions can be expected to be
424 very low in wintertime at Changchun, the presence of these compounds further underlines the
425 strong impact of anthropogenic emissions on CHOS− formation in Changchun−. In this study,
426 (O−3S)/C ratio was used instead of traditional O/C ratio to present the oxidation state of CHOS−
427 compounds, since the sulfate functional group contains three more oxygen atoms than common
428 oxygen-containing groups (e.g., hydroxyl and carbonyl), which makes no contribution to the
429 oxidation state of the carbon backbone of the CHOS− compounds. Comparing average values for
430 H/C, (O−3S)/C and DBEs of CHOS− for the three sample locations (see Table 1), we find that the
431 H/C ratios (1.85) and (O−3S)/C ratios (0.61−0.71) for Shanghai− and Guangzhou− samples are
432 larger than those for Changchun− samples (H/C = 1.56 and (O−3S)/C = 0.52), whereas the DBE
433 values (1.71−1.79) in Shanghai− and Guangzhou− are lower than those for Changchun− (2.55).
434 These observations indicate that CHOS− compounds in urban OA from Northeast China are less
435 oxidized but more unsaturated compared to those in East and Southeast China, likely due to
436 enhanced emissions from residential heating during winter in North China.

437 **3.6 CHONS compounds**

438 4-5% of the total organics detected in ESI− were identified as CHONS− compounds. In contrast,
439 CHONS+ compounds account merely for 0.3−1% of all organics detected in ESI+. The average
440 MM_{avg} of the CHONS− compounds for the three sample locations ranges from 214 to 293 Da,
441 generally showing larger molecular masses than compounds of any other class because of the likely
442 presence of both nitrate and sulfate functional groups. In total, only 8 common CHONS− formulas
443 were detected for all three sample locations, accounting for 8%, 58% and 56% of the CHONS−
444 peak abundance in Changchun−, Shanghai− and Guangzhou−, respectively. As already observed

https://doi.org/10.5194/acp-2019-908
Preprint. Discussion started: 11 November 2019
© Author(s) 2019. CC BY 4.0 License.

Atmospheric Chemistry and Physics Discussions

for other compound classes, these percentages imply that the CHONS− compounds in urban OA of Shanghai− and Guangzhou− exhibit a rather similar chemical composition, whereas such compounds are significantly different for Changchun−.

In the OA samples of Shanghai− and Guangzhou−, 78−87% of CHONS− formulas have 7 or more O atoms, allowing the assignment of one $-OSO_3H$ and one $-NO_3$ functional groups in the molecular structures, thus, classifying them as potential nitrooxy-organosulfates. In contrast to Shanghai− and Guangzhou−, only 26% of CHONS− compounds were assigned to such nitroooxy-organosulfates for Changchun−, indicating that most of the N atoms in the CHONS− compounds are present in a reduced oxidation state, e.g., in the form of amines. The average DBE and Xc values of CHONS− compounds in Shanghai− and Guangzhou− are 3.3−3.45 and 0.43−0.44, respectively. Again these values differ significantly for the Changchun− samples with an increased average DBE of 3.75 and an average Xc of 1.06, indicating that CHONS- compounds in Changchun− possess on average a higher degree of unsaturation and aromaticity compared to such compounds in Shanghai− and Guangzhou− samples. Interestingly, the compound with formula $C_{10}H_{17}O_7NS$ has the highest relative peak abundance (32%) in Shanghai− and Guangzhou−, whereas in Changchun− the compound with formula $C_2H_3O_4NS$ is dominant. $C_{10}H_{17}O_7NS$ has previously been identified as pinanediol mononitrate generated from α/β-pinene (Iinuma et al., 2007; Surratt et al., 2008; Lin et al., 2012b; Wang et al., 2017), while $C_2H_3O_4NS$ may be assigned as a cyanogroup-containing sulfate. This observation is comparable to our previous study (Wang et al., 2019a), which found that $C_{10}H_{17}O_7NS$ was dominant for CHONS− compounds in low-concentration aerosol samples collected in Beijing (China) and Mainz (Germany). Consistently, a $C_2H_3O_4NS$ compound had the highest abundance among CHONS− compounds in polluted Beijing aerosol samples. This agreement can be explained by the adjacent locations of Beijing (39.99° N, 116.39° E) and Changchun (43.54° N, 125.13° E) and similar residential heating patterns by coal combustion during wintertime. In conclusion, these results further demonstrate that the precursors for CHONS− compounds in Shanghai− and Guangzhou− are different from those in Changchun−, which is probably due to differences in anthropogenic emissions.

4 Conclusion

The molecular composition of the organic fraction of $PM_{2.5}$ samples collected in three Chinese megacities (Changchun, Shanghai and Guangzhou) was investigated using a UHPLC-Orbitrap mass spectrometer. In total, 416−769 (ESI−) and 687−2943 (ESI+) organic compounds were observed and separated into five subgroups: CHO, CHN, CHON, CHOS and CHONS. Specifically,

https://doi.org/10.5194/acp-2019-908
Preprint. Discussion started: 11 November 2019
© Author(s) 2019. CC BY 4.0 License.

Atmospheric Chemistry and Physics Discussions

139 common formulas were detected in ESI− and 168 common formulas in ESI+ for all sample locations, accounting for 78−87% and 65−90% in terms of peak abundance, respectively. Overall, we found that urban OA in Changchun, Shanghai and Guangzhou shows a quite similar chemical composition for organic compounds of high concentrations. The majority of these organic species was assigned to mono-aromatic or poly-aromatic compounds, indicating that anthropogenic emissions are the major source for urban OA in all three cities.

Despite the chemical similarity of the three sample locations for major organic compounds in urban OA, remarkable differences were found in chemical composition of the remaining particle constituents, in particular for OA samples from Changchun. In general, a larger amount of polyaromatics was observed for Changchun samples, most likely due to emissions from coal combustion during wintertime residential heating period. Moreover, the abundance-weighted average DBE and average Xc values of the total organic compounds in Changchun were found to be larger than those for Shanghai and Guangzhou, showing that organic compounds in Changchun possess a higher degree of unsaturation and aromaticity. For average H/C and O/C ratios a similar trend was observed. While average H/C and O/C ratios detected in ESI− were found to be highest for Guangzhou samples, significantly lower values were observed for Shanghai and Changchun samples, indicating that OA collected in lower latitude regions of China experiences more intense photochemical oxidation processes.

Author contributions. RJH, TH and KW conducted the study design. LY, HN, JG and MW collected the $PM_{2.5}$ filter samples. KW and YZ carried out the experimental work and data analysis. KW wrote the manuscript. KW, TH, RJH, M. Brüggemann, YZ, JH, M. Bilde and MG interpreted data and edited the manuscript. All authors commented on and discussed the manuscript.

Competing interests. The authors declare that they have no conflict of interest.

Acknowledgements. This study was supported by the National Natural Science Foundation of China (NSFC, Grant No. 41877408, and No. 91644219), the National Key Research and Development Program of China (No. 2017YFC0212701), and the German Research Foundation (Deutsche Forschungsgemeinschaft, DFG) under Grant No. INST 247/664-1 FUGG. K. Wang and Y. Zhang acknowledge the scholarship from Chinese Scholarship Council (CSC) and Max Plank Graduate Center with Johannes Gutenberg University of Mainz (MPGC) and thanks Prof. Ulrich Pöschl, Dr. Christopher J. Kampf and Dr. Yafang Cheng for their helpful suggestion on this study.

https://doi.org/10.5194/acp-2019-908
Preprint. Discussion started: 11 November 2019
© Author(s) 2019. CC BY 4.0 License.

Atmospheric Chemistry and Physics Discussions

References

An, Z., Huang, R. J., Zhang, R., Tie, X., Li, G., Cao, J., Zhou, W., Shi, Z., Han, Y., Gu, Z., and Ji, Y.: Severe haze in northern China: A synergy of anthropogenic emissions and atmospheric processes, Proc Natl Acad Sci U S A, 116, 8657-8666, 10.1073/pnas.1900125116, 2019.

Brüggemann, M., Poulain, L., Held, A., Stelzer, T., Zuth, C., Richters, S., Mutzel, A., van Pinxteren, D., Iinuma, Y., Katkevica, S., Rabe, R., Herrmann, H., and Hoffmann, T.: Real-time detection of highly oxidized organosulfates and BSOA marker compounds during the F-BEACh 2014 field study, Atmos. Chem. Phys., 17, 1453-1469, 10.5194/acp-17-1453-2017, 2017.

Brüggemann, M., van Pinxteren, D., Wang, Y., Yu, J. Z., and Herrmann, H.: Quantification of known and unknown terpenoid organosulfates in PM10 using untargeted LC–HRMS/MS: contrasting summertime rural Germany and the North China Plain, Environmental Chemistry, -, https://doi.org/10.1071/EN19089, 2019.

Claeys, M., Graham, B., Vas, G., Wang, W., Vermeylen, R., Pashynska, V., Cafmeyer, J., Guyon, P., Andre, M., Artaxo, P., and Maenhaut, W.: Formation of secondary organic aerosol through photooxidation of isoprene, Science, 303, 1173-1175, 10.1126/science.1092805, 2004.

Daellenbach, K. R., Kourtchev, I., Vogel, A. L., Bruns, E. A., Jiang, J., Petäjä, T., Jaffrezo, J.-L., Aksoyoglu, S., Kalberer, M., Baltensperger, U., El Haddad, I., and Prévôt, A. S. H.: Impact of anthropogenic and biogenic sources on the seasonal variation in the molecular composition of urban organic aerosols: a field and laboratory study using ultra-high-resolution mass spectrometry, Atmospheric Chemistry and Physics, 19, 5973-5991, 10.5194/acp-19-5973-2019, 2019.

Ding, X., Zhang, Y.-Q., He, Q.-F., Yu, Q.-Q., Shen, R.-Q., Zhang, Y., Zhang, Z., Lyu, S.-J., Hu, Q.-H., Wang, Y.-S., Li, L.-F., Song, W., and Wang, X.-M.: Spatial and seasonal variations of secondary organic aerosol from terpenoids over China, J. geophy. Res.-Atoms., 121, 14661-14678, doi:10.1002/2016JD025467, 2016.

Elzein, A., Dunmore, R. E., Ward, M. W., Hamilton, J. F., and Lewis, A. C.: Variability of polycyclic aromatic hydrocarbons and their oxidative derivatives in wintertime Beijing, China, Atmospheric Chemistry and Physics, 19, 8741-8758, 10.5194/acp-19-8741-2019, 2019.

Fleming, L. T., Lin, P., Laskin, A., Laskin, J., Weltman, R., Edwards, R. D., Arora, N. K., Yadav, A., Meinardi, S., Blake, D. R., Pillarisetti, A., Smith, K. R., and Nizkorodov, S. A.: Molecular composition of particulate matter emissions from dung and brushwood burning household cookstoves in Haryana, India, Atmos. Chem. Phys., 18, 2461-2480, 10.5194/acp-18-2461-2018, 2018.

Fu, P., Kawamura, K., Okuzawa, K., Aggarwal, S. G., Wang, G., Kanaya, Y., and Wang, Z.: Organic molecular compositions and temporal variations of summertime mountain aerosols over Mt. Tai, North China Plain, J. Geophy. Res., 113, 10.1029/2008jd009900, 2008.

Glasius, M., Hansen, A. M. K., Claeys, M., Henzing, J. S., Jedynska, A. D., Kasper-Giebl, A., Kistler, M., Kristensen, K., Martinsson, J., Maenhaut, W., Nøjgaard, J. K., Spindler, G., Stenström, K. E., Swietlicki, E., Szidat, S., Simpson, D., and Yttri, K. E.: Composition and sources of carbonaceous aerosols in Northern Europe during winter, Atmos. Environ., 173, 127-141, 10.1016/j.atmosenv.2017.11.005, 2018.

Hansen, A. M. K., Kristensen, K., Nguyen, Q. T., Zare, A., Cozzi, F., Noejgaard, J. K., Skov, H., Brandt, J., Christensen, J. H., Strom, J., Tunved, P., Krejci, R., and Glasius, M.: Organosulfates and organic acids in Arctic aerosols: speciation, annual variation and concentration levels, Atmos. Chem. Phys., 14, 7807-7823, https://doi.org/10.5194/acp-14-7807-2014, 2014.

Hansen, A. M. K., Hong, J., Raatikainen, T., Kristensen, K., Ylisirniö, A., Virtanen, A., Petäjä, T., Glasius, M., and Prisle, N. L.: Hygroscopic properties and cloud condensation nuclei activation of limonene-derived organosulfates and their mixtures with ammonium sulfate, Atmos. Chem. Phys., 15, 14071-14089, https://doi.org/10.5194/acp-15-14071-2015, 2015.

He, X., Huang, X. H. H., Chow, K. S., Wang, Q., Zhang, T., Wu, D., and Yu, J. Z.: Abundance and Sources of Phthalic Acids, Benzene-Tricarboxylic Acids, and Phenolic Acids in PM2.5 at Urban and Suburban Sites in Southern China, ACS Earth and Space Chemistry, 2, 147-158, 10.1021/acsearthspacechem.7b00131, 2018.

Ho, C. S., Lam, C. W. K., Chan, M. H. M., Cheung, R. C. K., Law, L. K., Suen, M. W. M., and Tai, H. L.: Electrospray ionisation mass spectrometry: principles and clinical application, Clin. Biochem. Rev., 24, 10, 2003.

Hoffmann, T., Huang, R. J., and Kalberer, M.: Atmospheric analytical chemistry, Anal. Chem., 83, 4649-

https://doi.org/10.5194/acp-2019-908
Preprint. Discussion started: 11 November 2019
© Author(s) 2019. CC BY 4.0 License.

Atmospheric Chemistry and Physics Discussions

4664, 10.1021/ac2010718, 2011.
Huang, G., Liu, Y., Shao, M., Li, Y., Chen, Q., Zheng, Y., Wu, Z., Liu, Y., Wu, Y., Hu, M., Li, X., Lu, S., Wang, C., Liu, J., Zheng, M., and Zhu, T.: Potentially Important Contribution of Gas-Phase Oxidation of Naphthalene and Methylnaphthalene to Secondary Organic Aerosol during Haze Events in Beijing, Environ Sci Technol, 53, 1235-1244, 10.1021/acs.est.8b04523, 2019.
Huang, R. J., Zhang, Y., Bozzetti, C., Ho, K. F., Cao, J. J., Han, Y., Daellenbach, K. R., Slowik, J. G., Platt, S. M., Canonaco, F., Zotter, P., Wolf, R., Pieber, S. M., Bruns, E. A., Crippa, M., Ciarelli, G., Piazzalunga, A., Schwikowski, M., Abbaszade, G., Schnelle-Kreis, J., Zimmermann, R., An, Z., Szidat, S., Baltensperger, U., El Haddad, I., and Prevot, A. S.: High secondary aerosol contribution to particulate pollution during haze events in China, Nature, 514, 218-222, 10.1038/nature13774, 2014.
Huang, R. J., Cao, J. J., and Worsnop, D.: Sources and Chemical Composition of Particulate Matter During Haze Pollution Events in China, in: Air pollution in Eastern Asia: an integrated perspective, edited by Bouarar, I., Wang, X. M., and Brasseur, G. P., Springer, Cham, Switzerland, 49-68, 2017.
Iinuma, Y., Müller, C., Berndt, T., Böge, O., Claeys, M., and Herrmann, H.: Evidence for the existence of organosulfates from β-pinene ozonolysis in ambient secondary organic aerosol, Environ. Sci. Technol., 41, 6678-6683, 10.1021/es070938t, 2007.
Jung, J., and Kawamura, K.: Enhanced concentrations of citric acid in spring aerosols collected at the Gosan background site in East Asia, Atmos. Environ., 45, 5266-5272, 10.1016/j.atmosenv.2011.06.065, 2011.
Kautzman, K. E., Surratt, J. D., Chan, M. N., Chan, A. W., Hersey, S. P., Chhabra, P. S., Dalleska, N. F., Wennberg, P. O., Flagan, R. C., and Seinfeld, J. H.: Chemical composition of gas- and aerosol-phase products from photooxidation of naphthalene, J. Phys. Chem. A, 114, 913-934, 10.1021/jp908530s, 2010.
Kind, T., and Fiehn, O.: Seven Golden Rules for heuristic filtering of molecular formulas obtained by accurate mass spectrometry, BMC Bioinformatics, 8, 10.1186/1471-2105-8-105, 2007.
Kourtchev, I., O'Connor, I. P., Giorio, C., Fuller, S. J., Kristensen, K., Maenhaut, W., Wenger, J. C., Sodeau, J. R., Glasius, M., and Kalberer, M.: Effects of anthropogenic emissions on the molecular composition of urban organic aerosols: An ultrahigh resolution mass spectrometry study, Atmo. Environ., 89, 525-532, 10.1016/j.atmosenv.2014.02.051, 2014.
Kourtchev, I., Godoi, R. H. M., Connors, S., Levine, J. G., Archibald, A. T., Godoi, A. F. L., Paralovo, S. L., Barbosa, C. G. G., Souza, R. A. F., Manzi, A. O., Seco, R., Sjostedt, S., Park, J.-H., Guenther, A., Kim, S., Smith, J., Martin, S. T., and Kalberer, M.: Molecular composition of organic aerosols in central Amazonia: an ultra-high-resolution mass spectrometry study, Atmos. Chem. Phys., 16, 11899-11913, https://doi.org/10.5194/acp-16-11899-2016, 2016.
Laskin, A., Laskin, J., and Nizkorodov, S. A.: Chemistry of atmospheric brown carbon, Chem. Rev., 115, 4335-4382, 10.1021/cr5006167, 2015.
Laskin, J., Laskin, A., Roach, P. J., Slysz, G. W., Anderson, G. A., Nizkorodov, S. A., Bones, D. L., and Nguyen, L. Q.: High-Resolution Desorption Electrospray Ionization Mass Spectrometry for Chemical Characterization of Organic Aerosols, Anal. Chem., 82, 2048-2058, 10.1021/ac902801f, 2010.
Laskin, J., Laskin, A., and Nizkorodov, S. A.: Mass Spectrometry Analysis in Atmospheric Chemistry, Anal. Chem., 90, 166-189, 10.1021/acs.analchem.7b04249, 2018.
Lee, A., Goldstein, A. H., Kroll, J. H., Ng, N. L., Varutbangkul, V., Flagan, R. C., and Seinfeld, J. H.: Gas-phase products and secondary aerosol yields from the photooxidation of 16 different terpenes, J. Geophy. Res., 111, 10.1029/2006jd007050, 2006.
Lim, Y. B., Tan, Y., Perri, M. J., Seitzinger, S. P., and Turpin, B. J.: Aqueous chemistry and its role in secondary organic aerosol (SOA) formation, Atmos. Chem. Phys., 10, 10521-10539, 10.5194/acp-10-10521-2010, 2010.
Lin, P., Rincon, A. G., Kalberer, M., and Yu, J. Z.: Elemental composition of HULIS in the Pearl River Delta Region, China: results inferred from positive and negative electrospray high resolution mass spectrometric data, Environ. Sci. Technol., 46, 7454-7462, 10.1021/es300285d, 2012a.
Lin, P., Yu, J. Z., Engling, G., and Kalberer, M.: Organosulfates in humic-like substance fraction isolated from aerosols at seven locations in East Asia: a study by ultra-high-resolution mass spectrometry, Environ. Sci. Technol., 46, 13118-13127, 10.1021/es303570v, 2012b.
Lin, P., Laskin, J., Nizkorodov, S. A., and Laskin, A.: Revealing Brown Carbon Chromophores Produced in Reactions of Methylglyoxal with Ammonium Sulfate, Environ. Sci. Technol., 49, 14257-14266, 10.1021/acs.est.5b03608, 2015.
McNeill, V. F., Woo, J. L., Kim, D. D., Schwier, A. N., Wannell, N. J., Sumner, A. J., and Barakat, J. M.:

https://doi.org/10.5194/acp-2019-908
Preprint. Discussion started: 11 November 2019
© Author(s) 2019. CC BY 4.0 License.

Atmospheric Chemistry and Physics Discussions

Aqueous-phase secondary organic aerosol and organosulfate formation in atmospheric aerosols: a modeling study, Environ Sci Technol, 46, 8075-8081, 10.1021/es3002986, 2012.

Ning, C., Gao, Y., Zhang, H., Yu, H., Wang, L., Geng, N., Cao, R., and Chen, J.: Molecular characterization of dissolved organic matters in winter atmospheric fine particulate matters (PM2.5) from a coastal city of northeast China, Sci Total Environ, 689, 312-321, 10.1016/j.scitotenv.2019.06.418, 2019.

Nizkorodov, S. A., Laskin, J., and Laskin, A.: Molecular chemistry of organic aerosols through the application of high resolution mass spectrometry, Phys. Chem. Chem. Phys., 13, 3612-3629, 10.1039/c0cp02032j, 2011.

Noziere, B., Kalberer, M., Claeys, M., Allan, J., D'Anna, B., Decesari, S., Finessi, E., Glasius, M., Grgic, I., Hamilton, J. F., Hoffmann, T., Iinuma, Y., Jaoui, M., Kahnt, A., Kampf, C. J., Kourtchev, I., Maenhaut, W., Marsden, N., Saarikoski, S., Schnelle-Kreis, J., Surratt, J. D., Szidat, S., Szmigielski, R., and Wisthaler, A.: The molecular identification of organic compounds in the atmosphere: state of the art and challenges, Chem. Rev., 115, 3919-3983, 10.1021/cr5003485, 2015.

Pereira, K. L., Hamilton, J. F., Rickard, A. R., Bloss, W. J., Alam, M. S., Camredon, M., Muñoz, A., Vázquez, M., Borrás, E., and Ródenas, M.: Secondary organic aerosol formation and composition from the photo-oxidation of methyl chavicol (estragole), Atmos. Chem. Phys., 14, 5349-5368, 10.5194/acp-14-5349-2014, 2014.

Perry, R. H., Cooks, R. G., and Noll, R. J.: ORBITRAP MASS SPECTROMETRY: INSTRUMENTATION, ION MOTION AND APPLICATIONS, Mass Spectrometry Reviews, 27, 661-699, 10.1002/mas.20186, 2008.

Rincón, A. G., Calvo, A. I., Dietzel, M., and Kalberer, M.: Seasonal differences of urban organic aerosol composition - an ultra-high resolution mass spectrometry study, Environ. Chem., 9, 298, 10.1071/en12016, 2012.

Riva, M., Tomaz, S., Cui, T., Lin, Y.-H., Perraudin, E., Gold, A., Stone, E. A., Villenave, E., and Surratt, J. D.: Evidence for an Unrecognized Secondary Anthropogenic Source of Organosulfates and Sulfonates: Gas-Phase Oxidation of Polycyclic Aromatic Hydrocarbons in the Presence of Sulfate Aerosol, Environ. Sci. Technol., 49, 6654-6664, 10.1021/acs.est.5b00836, 2015.

Shi, Z., Vu, T., Kotthaus, S., Harrison, R. M., Grimmond, S., Yue, S., Zhu, T., Lee, J., Han, Y., Demuzere, M., Dunmore, R. E., Ren, L., Liu, D., Wang, Y., Wild, O., Allan, J., Acton, W. J., Barlow, J., Barratt, B., Beddows, D., Bloss, W. J., Calzolai, G., Carruthers, D., Carslaw, D. C., Chan, Q., Chatzidiakou, L., Chen, Y., Crilley, L., Coe, H., Dai, T., Doherty, R., Duan, F., Fu, P., Ge, B., Ge, M., Guan, D., Hamilton, J. F., He, K., Heal, M., Heard, D., Hewitt, C. N., Hollaway, M., Hu, M., Ji, D., Jiang, X., Jones, R., Kalberer, M., Kelly, F. J., Kramer, L., Langford, B., Lin, C., Lewis, A. C., Li, J., Li, W., Liu, H., Liu, J., Loh, M., Lu, K., Lucarelli, F., Mann, G., McFiggans, G., Miller, M. R., Mills, G., Monk, P., Nemitz, E., amp, apos, Connor, F., Ouyang, B., Palmer, P. I., Percival, C., Popoola, O., Reeves, C., Rickard, A. R., Shao, L., Shi, G., Spracklen, D., Stevenson, D., Sun, Y., Sun, Z., Tao, S., Tong, S., Wang, Q., Wang, W., Wang, X., Wang, X., Wang, Z., Wei, L., Whalley, L., Wu, X., Wu, Z., Xie, P., Yang, F., Zhang, Q., Zhang, Y., Zhang, Y., and Zheng, M.: Introduction to the special issue "In-depth study of air pollution sources and processes within Beijing and its surrounding region (APHH-Beijing)", Atmospheric Chemistry and Physics, 19, 7519-7546, 10.5194/acp-19-7519-2019, 2019.

Song, J., Li, M., Jiang, B., Wei, S., Fan, X., and Peng, P.: Molecular Characterization of Water-Soluble Humic like Substances in Smoke Particles Emitted from Combustion of Biomass Materials and Coal Using Ultrahigh-Resolution Electrospray Ionization Fourier Transform Ion Cyclotron Resonance Mass Spectrometry, Environ. Sci. Technol., 52, 2575-2585, 10.1021/acs.est.7b06126, 2018.

Sun, Y., Jiang, Q., Zhang, Z., Fu, P., Li, J., Yang, T., and Yin, Y.: Investigation of the sources and evolution processes of severe haze pollution in Beijing in January 2013, J. Geophy. Res.-Atmos., 119, 4380-4389, 10.1002/, 2014.

Surratt, J. D., Gomez-Gonzalez, Y., Chan, A. W., Vermeylen, R., Shahgholl, M., Kleindienst, T. E., Jaoui, M., Maenhaut, W., Claeys, M., Flagan, R. C., and Seinfeld, J. H.: Evidence for Organosulfate in Secondary Organic Aerosol, Environ. Sci. Technol., 41, 517-527, 10.1021/es062081q, 2007.

Surratt, J. D., Gómez-González, Y., Chan, A. W., Vermeylen, R., Shahgholi, M., Kleindienst, T. E., Edney, E. O., Offenberg, J. H., Lewandowski, M., Jaoui, M., Maenhaut, W., Claeys, M., Flagan, R. C., and Seinfeld, J. H.: Organosulfate Formation in Biogenic Secondary Organic Aerosol, J. Phys. Chem. A, 112, 8345-8378, 2008.

Tao, S., Lu, X., Levac, N., Bateman, A. P., Nguyen, T. B., Bones, D. L., Nizkorodov, S. A., Laskin, J., Laskin,

© Author(s) 2019. CC BY 4.0 License.

674 A., and Yang, X.: Molecular Characterization of Organosulfates in Organic Aerosols from Shanghai and
675 Los Angeles Urban Areas by Nanospray-Desorption Electrospray Ionization High-Resolution Mass
676 Spectrometry, Environ. Sci. Technol., 48, 10993-11001, 10.1021/es5024674, 2014.
677 Tong, H., Kourtchev, I., Pant, P., Keyte, I. J., O'Connor, I. P., Wenger, J. C., Pope, F. D., Harrison, R. M.,
678 and Kalberer, M.: Molecular composition of organic aerosols at urban background and road tunnel sites
679 using ultra-high resolution mass spectrometry, Faraday Discuss., 189, 51-68, 10.1039/c5fd00206k, 2016.
680 Tu, P., Hall, W. A. t., and Johnston, M. V.: Characterization of Highly Oxidized Molecules in Fresh and
681 Aged Biogenic Secondary Organic Aerosol, Anal. Chem., 88, 4495-4501,
682 10.1021/acs.analchem.6b00378, 2016.
683 Wang, G., Kawamura, K., Umemoto, N., Xie, M., Hu, S., and Wang, Z.: Water-soluble organic compounds
684 in PM2.5and size-segregated aerosols over Mount Tai in North China Plain, J. Geophy. Res., 114,
685 10.1029/2008jd011390, 2009.
686 Wang, K., Zhang, Y., Huang, R.-J., Cao, J., and Hoffmann, T.: UHPLC-Orbitrap mass spectrometric
687 characterization of organic aerosol from a central European city (Mainz, Germany) and a Chinese
688 megacity (Beijing), Atmos. Environ., 189, 22-29, 10.1016/j.atmosenv.2018.06.036, 2018.
689 Wang, K., Zhang, Y., Huang, R.-J., Wang, M., Ni, H., Kampf, C. J., Cheng, Y., Bilde, M., Glasius, M., and
690 Hoffmann, T.: Molecular characterization and source identification of atmospheric particulate
691 organosulfates using ultrahigh resolution mass spectrometry, Environ. Sci. Technol.,
692 10.1021/acs.est.9b02628, 2019a.
693 Wang, M., Huang, R.-J., Cao, J., Dai, W., Zhou, J., Lin, C., Ni, H., Duan, J., Wang, T., Chen, Y., Li, Y.,
694 Chen, Q., Haddad, I. E., and Hoffmann, T.: Determination of n-alkanes, PAHs and hopanes in
695 atmospheric aerosol: evaluation and comparison of thermal desorption GC-MS and solvent extraction
696 GC-MS approaches, Atmos. Mea. Tech. Discuss., 1-21, 10.5194/amt-2019-4, 2019b.
697 Wang, X. K., Rossignol, S., Ma, Y., Yao, L., Wang, M. Y., Chen, J. M., George, C., and Wang, L.: Molecular
698 characterization of atmospheric particulate organosulfates in three megacities at the middle and lower
699 reaches of the Yangtze River, Atmos. Chem. Phys., 16, 2285-2298, https://doi.org/10.5194/acp-16-2285-
700 2016, 2016.
701 Wang, X. K., Hayeck, N., Brüggemann, M., Yao, L., Chen, H. F., Zhang, C., Emmelin, C., Chen, J. M.,
702 George, C., and Wang, L.: Chemical characterization of organic aerosol in: A study by Ultrahigh-
703 Performance Liquid Chromatography Coupled with Orbitrap Mass Spectrometry, J. Geophy. Res.-Atmos.,
704 122, 703-722, https://doi.org/10.1002/2017JD026930, 2017.
705 Xu, W., Sun, Y., Wang, Q., Zhao, J., Wang, J., Ge, X., Xie, C., Zhou, W., Du, W., Li, J., Fu, P., Wang, Z.,
706 Worsnop, D. R., and Coe, H.: Changes in Aerosol Chemistry From 2014 to 2016 in Winter in Beijing:
707 Insights From High-Resolution Aerosol Mass Spectrometry, J. Geophy. Res.-Atmos., 124, 1132-1147,
708 10.1029/2018jd029245, 2019.
709 Yassine, M. M., Harir, M., Dabek-Zlotorzynska, E., and Schmitt-Kopplin, P.: Structural characterization of
710 organic aerosol using Fourier transform ion cyclotron resonance mass spectrometry: aromaticity
711 equivalent approach, Rapid Commun. Mass Spectrom., 28, 2445-2454, 10.1002/rcm.7038, 2014.
712 Zielinski, A. T., Kourtchev, I., Bortolini, C., Fuller, S. J., Giorio, C., Popoola, O. A. M., Bogialli, S., Tapparo,
713 A., Jones, R. L., and Kalberer, M.: A new processing scheme for ultra-high resolution direct infusion
714 mass spectrometry data, Atmos. Environ., 178, 129-139, 10.1016/j.atmosenv.2018.01.034, 2018.

715

716

717

718

719

720

https://doi.org/10.5194/acp-2019-908
Preprint. Discussion started: 11 November 2019
© Author(s) 2019. CC BY 4.0 License.

Atmospheric Chemistry and Physics Discussions

721 **Table legend**

722 Table 1: Number of organic compounds in each subgroup and the abundance-weighted average
723 values of molecular mass (MM_{avg}), elemental ratios, double bond equivalent (DBE) and
724 aromaticity equivalent (Xc) for detected organic compounds in ESI− and ESI+ in the three Chinese
725 cities.

726 **Figure legends**

727 Figure 1: Mass spectra of detected organic compounds reconstructed from extracted ion
728 chromatograms in ESI− and ESI+. X axis refers to the molecular mass (Da) of the identified species.
729 Y axis refers to the relative peak abundance of each individual compound to the compound with
730 the greatest peak abundance. The pie charts show the percentage of each organic compound
731 subgroup (i.e., CHO, CHON, CHOS, CHONS and CHN) in each sample in terms of peak
732 abundance. The map in the lower right corner shows the locations of these three megacities in China.

733 Figure 2: (a) Venn diagrams showing the number distribution of all molecular formulas detected in
734 ESI− and ESI+ for all sample locations. (b) Peak abundance contribution of each elemental formula
735 category to the total common formulas.

736 Figure 3: Double bond equivalent (DBE) versus carbon number for all CHO− compounds for all
737 sample locations. The molecular formula represents the abundance-weighted average CHO−
738 formula and the area of the circles is proportional to the fourth root of the peak abundance of an
739 individual compound. The color bar denotes the aromaticity equivalent (gray with $Xc < 2.50$, purple
740 with $2.50 \leq Xc < 2.70$ and red with $Xc \geq 2.70$). The pie charts show the percentage of each Xc
741 category (i.e., gray color-coded compounds, purple color-coded compounds and red color-coded
742 compounds) in each sample in terms of peak abundance.

743 Figure 4: Classification of CHON− compounds into different subgroups according to O/N ratios in
744 their formulas. The y-axis indicates the relative contribution of each specific O/N ratio subgroup to
745 the sum of peak abundances of CHON− compounds.

746 Figure 5: Double bond equivalent (DBE) versus carbon number for all CHON− compounds for all
747 sample locations. The molecular formula represents the abundance-weighted average CHON-
748 formula and the area of circles is proportional to the fourth root of the peak abundance of an
749 individual compound. The color bar denotes the aromaticity equivalent (gray with $XC < 2.50$,
750 purple with $2.50 \leq XC < 2.70$ and red with $XC \geq 2.70$). The pie charts show the percentage of each
751 Xc category (i.e., gray color-coded compounds, purple color-coded compounds and red color-
752 coded compounds) in each sample in terms of peak abundance.

753 Figure 6: Van Krevelen diagrams for CHN+ compounds in Changchun, Shanghai and Guangzhou
754 samples. The area of circles is proportional to the fourth root of the peak abundance of an individual
755 compound and the color bar denotes the aromaticity equivalent (gray with $Xc < 2.50$, purple with
756 $2.50 \leq Xc < 2.70$ and red with $Xc \geq 2.70$). The pie charts show the percentage of each Xc category
757 (i.e., gray color-coded compounds, purple color-coded compounds and red color-coded compounds)
758 in each sample in terms of peak abundance.

759 Figure 7: Double bond equivalent (DBE) versus carbon number for all CHOS− compounds for all
760 sample locations. The molecular formula represents the abundance-weighted average CHOS−
761 formula and the area of circles is proportional to the fourth root of the peak abundance of an
762 individual compound. The color bar denotes the aromaticity equivalent (gray with $Xc < 2.50$, purple
763 with $2.50 \leq Xc < 2.70$ and red with $Xc \geq 2.70$). The pie charts show the percentage of each Xc
764 category (i.e., gray color-coded compounds, purple color-coded compounds and red color-coded

https://doi.org/10.5194/acp-2019-908
Preprint. Discussion started: 11 November 2019
© Author(s) 2019. CC BY 4.0 License.

Atmospheric Chemistry and Physics Discussions

765 compounds) in each sample in terms of peak abundance.

766

767

768

769

770

771

772

773

774

775

776

777

778

779

780

781

782

783

784

785

786

787

788

789

790

791

792

793

794

https://doi.org/10.5194/acp-2019-908
Preprint. Discussion started: 11 November 2019
© Author(s) 2019. CC BY 4.0 License.

Atmospheric Chemistry and Physics Discussions

Table 1. Number of organic compounds in each subgroup and the abundance-weighted average values of molecular mass (MM_{avg}), elemental ratios, double bond equivalent (DBE) and aromaticity equivalent (Xc) for detected organic compounds in ESI− and ESI+ in the three Chinese cities.

Sample ID	Subgroup	Number of compounds	Relative abundance (%)	MM_{avg}	H/C	O/C*	DBE	Xc
Changchun−	total	769	100	169	1.03	0.58	5.02	2.13
	CHO−	346	30	162	0.96	0.41	5.65	2.28
	CHON−	180	55	163	0.94	0.51	5.24	2.44
	CHOS−	155	10	198	1.56	1.17(0.52)	2.55	0.50
	CHONS−	88	5	214	1.35	1.07(-1.4)	3.75	1.06
Shanghai−	total	416	100	176	1.05	0.69	4.99	1.92
	CHO−	164	40	171	0.97	0.59	5.37	1.94
	CHON−	135	44	169	0.86	0.56	5.67	2.47
	CHOS−	75	12	190	1.85	1.41(0.61)	1.79	0.34
	CHONS−	42	4	266	1.56	1.00(0.11)	3.30	0.44
Guangzhou−	total	488	100	183	1.14	0.74	4.55	1.65
	CHO−	196	42	172	1.10	0.65	4.68	1.57
	CHON−	161	39	173	0.89	0.58	5.56	2.41
	CHOS−	86	14	201	1.85	1.48(0.71)	1.71	0.21
	CHONS−	45	5	293	1.56	0.82(0.06)	3.45	0.43
Changchun+	total	2943	100	160	1.21	0.13	5.58	2.36
	CHO+	609	13	174	0.94	0.28	6.55	2.22
	CHN+	696	40	154	1.22	0.00	5.84	2.60
	CHON+	1594	46.5	161	1.27	0.19	5.11	2.22
	CHONS+	44	0.5	196	1.91	0.70	2.64	0.09
Shanghai+	total	704	100	162	1.37	0.09	4.91	2.32
	CHO+	87	4	184	1.13	0.43	5.46	1.46
	CHN+	253	71	159	1.38	0.00	5.08	2.55
	CHON+	350	24.7	167	1.40	0.27	4.34	1.81
	CHONS+	14	0.3	241	1.17	0.61	5.32	0.91
Guangzhou+	total	687	100	161	1.41	0.17	4.58	2.07
	CHO+	125	8	185	1.12	0.42	5.19	1.20
	CHN+	205	62	156	1.42	0.00	4.80	2.47
	CHON+	336	29	165	1.47	0.45	4.00	1.51
	CHONS+	21	1	209	1.84	0.71	3.05	0.31

*The values in brackets indicate the (O−3S)/C and (O−3S−2N)/C ratios for CHOS and CHONS compounds, respectively, detected in ESI− mode.

https://doi.org/10.5194/acp-2019-908
Preprint. Discussion started: 11 November 2019
© Author(s) 2019. CC BY 4.0 License.

Atmospheric Chemistry and Physics Discussions

804

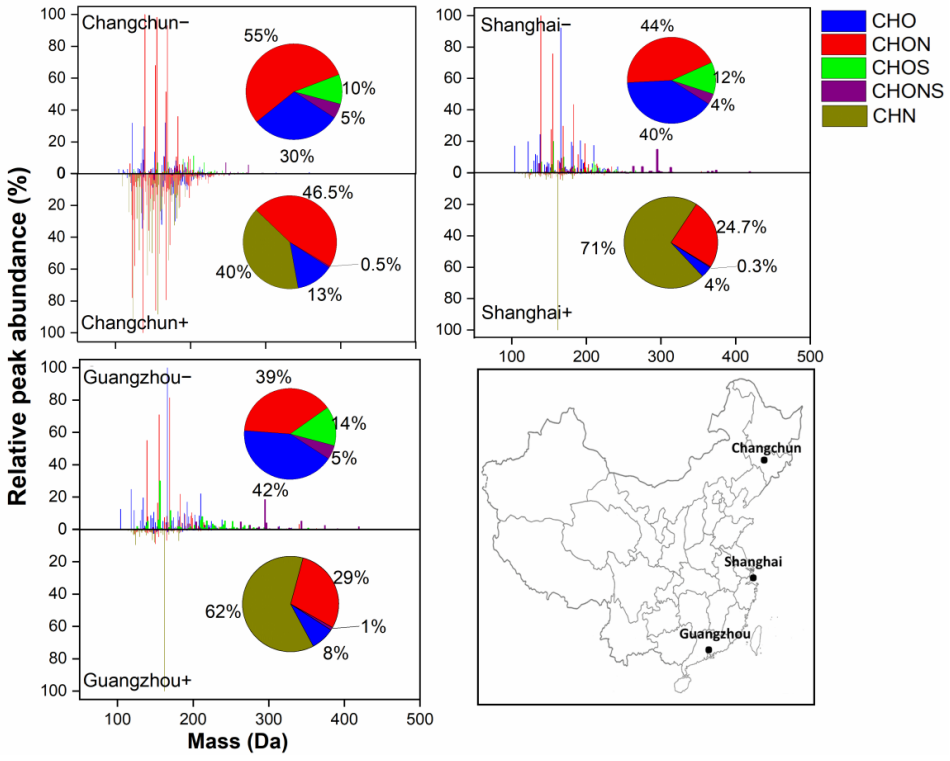

805
806 Figure 1. Mass spectra of detected organic compounds reconstructed from extracted ion
807 chromatograms in ESI− and ESI+. X axis refers to the molecular mass (Da) of the identified species.
808 Y axis refers to the relative peak abundance of each individual compound to the compound with
809 the greatest peak abundance. The pie charts show the percentage of each organic compound
810 subgroup (i.e., CHO, CHON, CHOS, CHONS and CHN) in each sample in terms of peak
811 abundance. The map in the lower right corner shows the locations of these three megacities in China.

https://doi.org/10.5194/acp-2019-908
Preprint. Discussion started: 11 November 2019
© Author(s) 2019. CC BY 4.0 License.

Atmospheric Chemistry and Physics Discussions

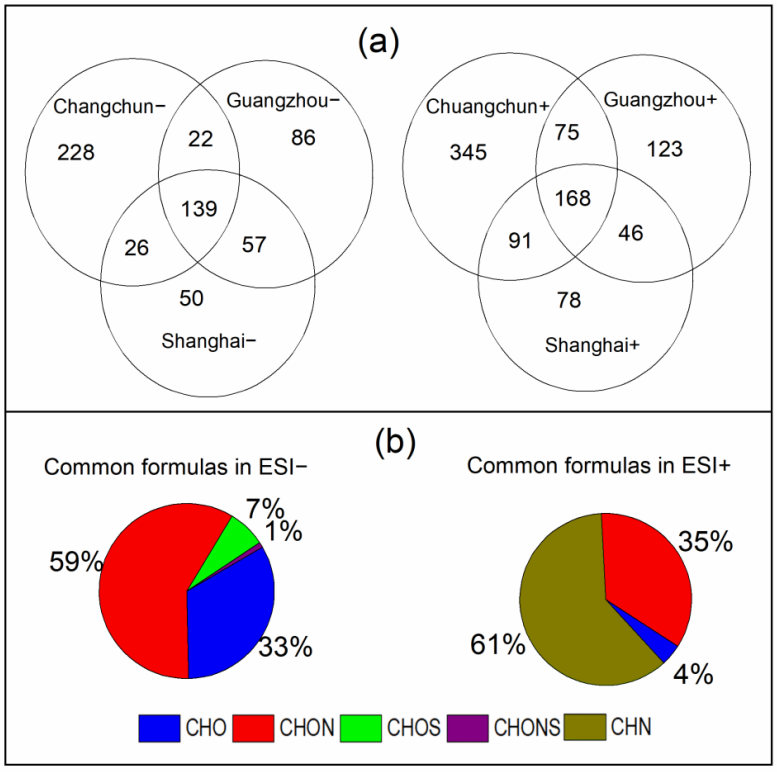

812

813 Figure 2. (a) Venn diagrams showing the number distribution of all molecular formulas detected in
814 ESI− and ESI+ for all sample locations. (b) Peak abundance contribution of each elemental formula
815 category to the total common formulas.

https://doi.org/10.5194/acp-2019-908
Preprint. Discussion started: 11 November 2019
© Author(s) 2019. CC BY 4.0 License.

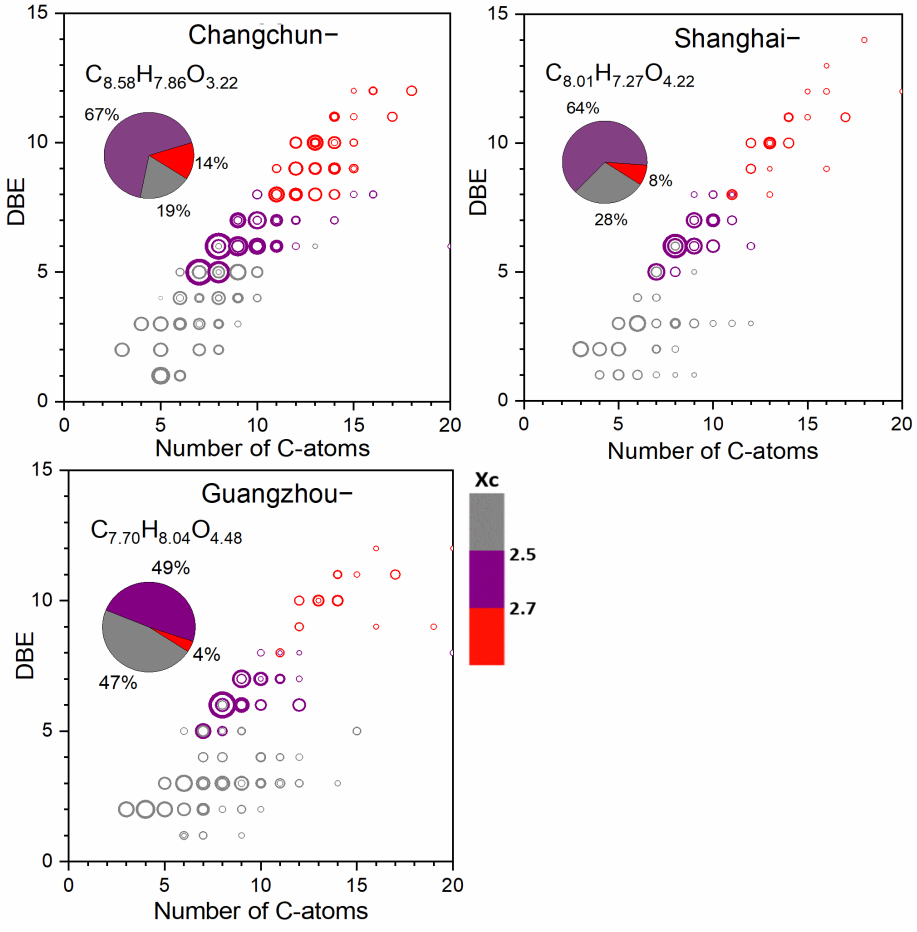

Figure 3. Double bond equivalent (DBE) versus carbon number for all CHO− compounds for all sample locations. The molecular formula represents the abundance-weighted average CHO− formula and the area of the circles is proportional to the fourth root of the peak abundance of an individual compound. The color bar denotes the aromaticity equivalent (gray with Xc < 2.50, purple with 2.50 ≤ Xc < 2.70 and red with Xc ≥ 2.70). The pie charts show the percentage of each Xc category (i.e., gray color-coded compounds, purple color-coded compounds and red color-coded compounds) in each sample in terms of peak abundance.

https://doi.org/10.5194/acp-2019-908
Preprint. Discussion started: 11 November 2019
© Author(s) 2019. CC BY 4.0 License.

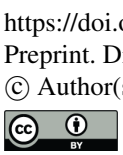

Atmospheric Chemistry and Physics Discussions

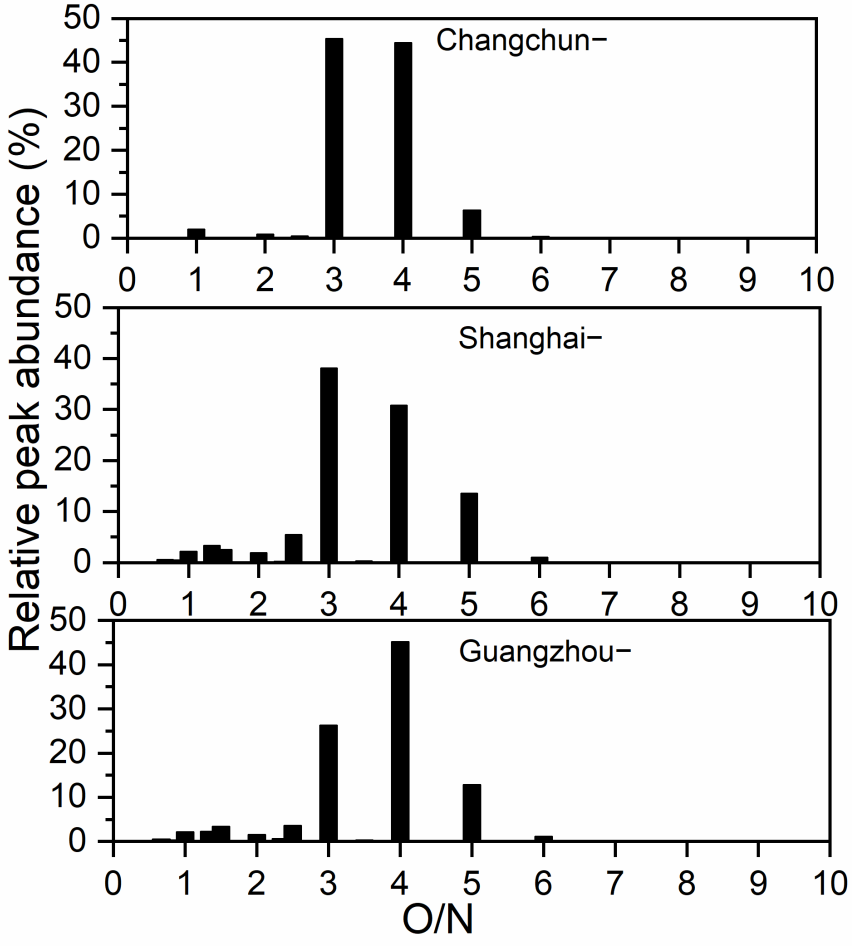

Figure 4. Classification of CHON− compounds into different subgroups according to O/N ratios in their formulas. The y-axis indicates the relative contribution of each specific O/N ratio subgroup to the sum of peak abundances of CHON− compounds.

https://doi.org/10.5194/acp-2019-908
Preprint. Discussion started: 11 November 2019
© Author(s) 2019. CC BY 4.0 License.

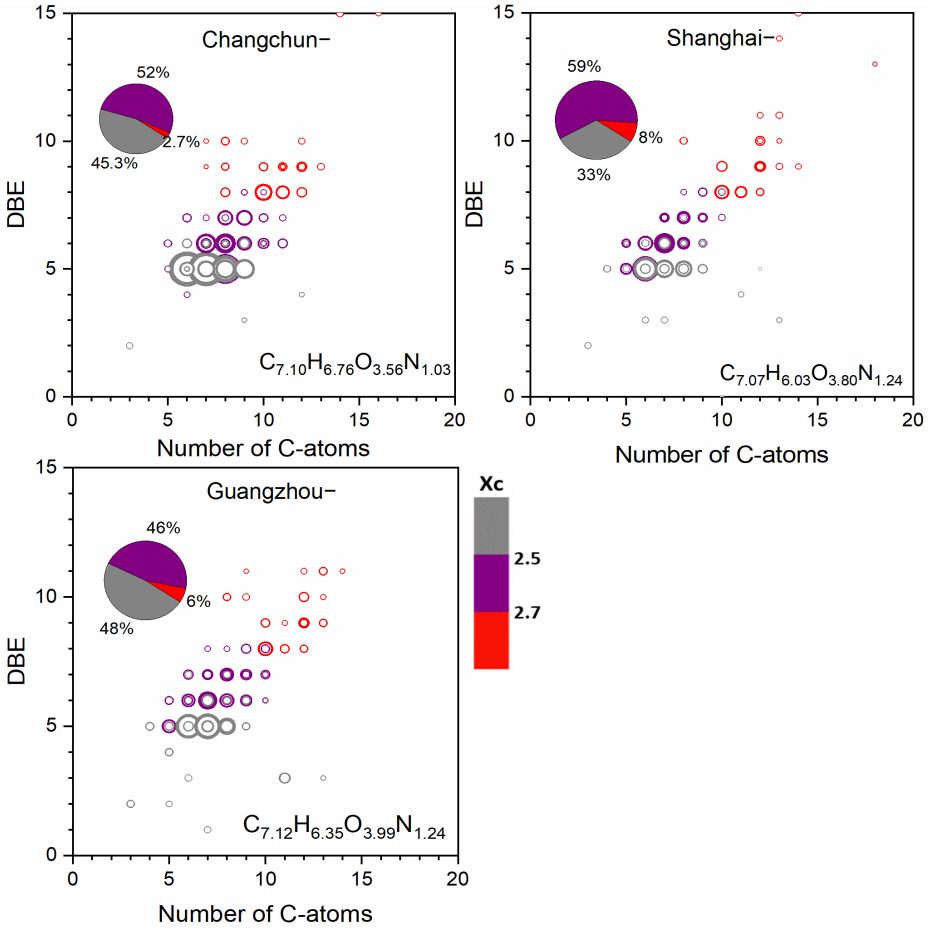

Figure 5. Double bond equivalent (DBE) versus carbon number for all CHON− compounds for all sample locations. The molecular formula represents the abundance-weighted average CHON- formula and the area of circles is proportional to the fourth root of the peak abundance of an individual compound. The color bar denotes the aromaticity equivalent (gray with XC < 2.50, purple with 2.50 ≤ XC < 2.70 and red with XC ≥ 2.70). The pie charts show the percentage of each Xc category (i.e., gray color-coded compounds, purple color-coded compounds and red color-coded compounds) in each sample in terms of peak abundance.

https://doi.org/10.5194/acp-2019-908
Preprint. Discussion started: 11 November 2019
© Author(s) 2019. CC BY 4.0 License.

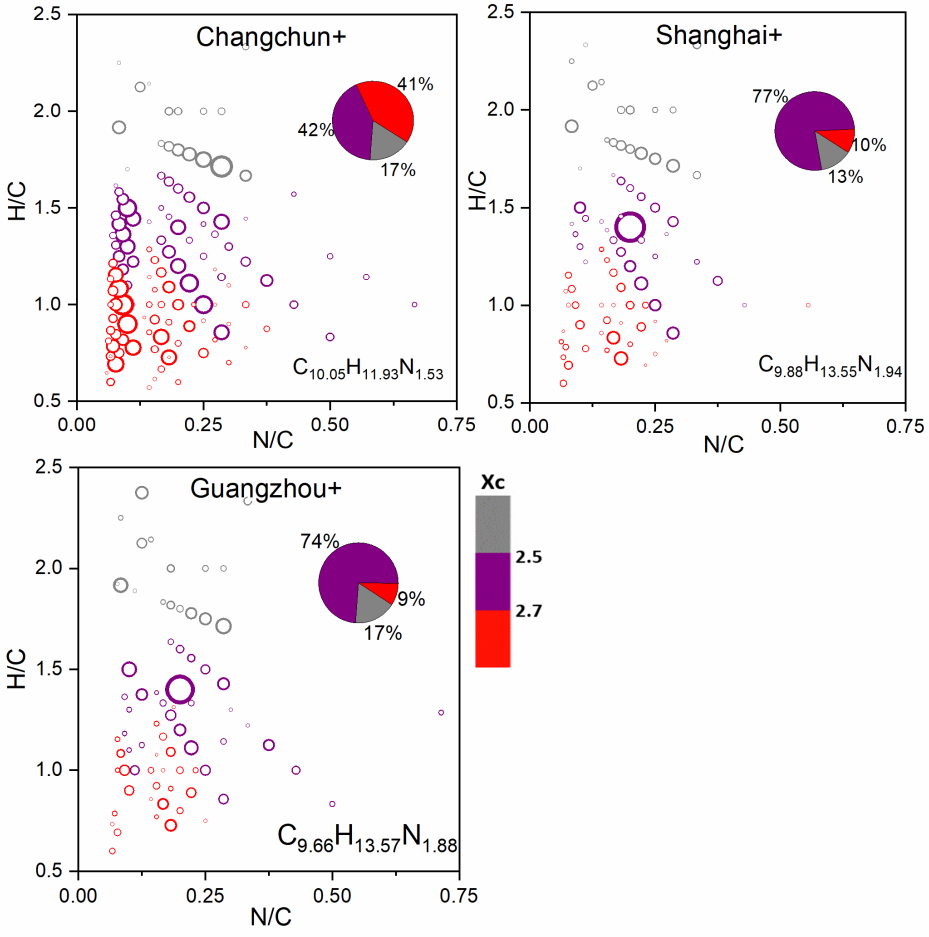

Figure 6. Van Krevelen diagrams for CHN+ compounds in Changchun, Shanghai and Guangzhou samples. The area of circles is proportional to the fourth root of the peak abundance of an individual compound and the color bar denotes the aromaticity equivalent (gray with Xc < 2.50, purple with 2.50 ≤ Xc < 2.70 and red with Xc ≥ 2.70). The pie charts show the percentage of each Xc category (i.e., gray color-coded compounds, purple color-coded compounds and red color-coded compounds) in each sample in terms of peak abundance.

https://doi.org/10.5194/acp-2019-908
Preprint. Discussion started: 11 November 2019
© Author(s) 2019. CC BY 4.0 License.

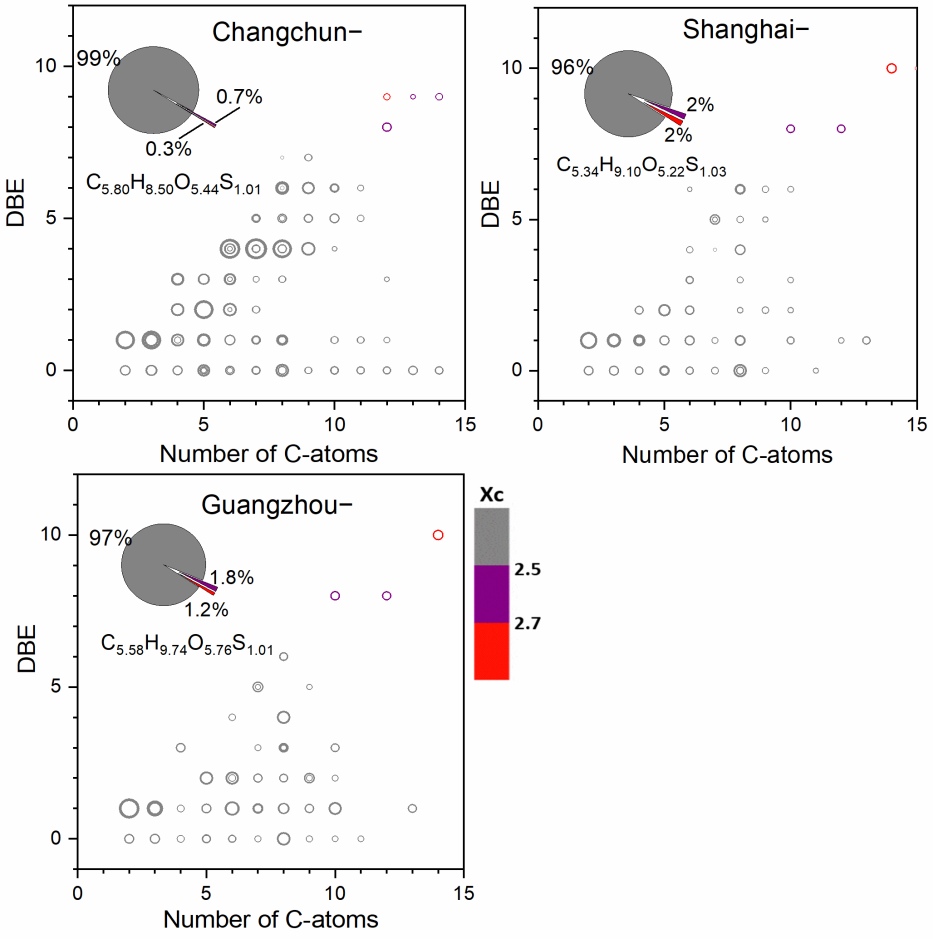

Figure 7. Double bond equivalent (DBE) versus carbon number for all CHOS− compounds for all sample locations. The molecular formula represents the abundance-weighted average CHOS− formula and the area of circles is proportional to the fourth root of the peak abundance of an individual compound. The color bar denotes the aromaticity equivalent (gray with Xc < 2.50, purple with 2.50 ≤ Xc < 2.70 and red with Xc ≥ 2.70). The pie charts show the percentage of each Xc category (i.e., gray color-coded compounds, purple color-coded compounds and red color-coded compounds) in each sample in terms of peak abundance.